Available online at www.sciencedirect.com

SCIENCE DIRECT

European Journal of Pharmacology 514 (2005) 1 – 15

www.elsevier.com/locate/ejphar

Inhibition of angiogenesis and tumor growth by β and γ-secretase inhibitors

Daniel Paris*, Amita Quadros, Nikunj Patel, Anthony DelleDonne, James Humphrey, Michael Mullan

The Roskamp Institute, 2040 Whitfield Avenue, Sarasota, FL 34243, USA

Received 17 February 2005; accepted 25 February 2005

Abstract

The involvement of β-secretase and γ-secretase in producing the β-amyloid component of senile plaques found in the brain of Alzheimer's patients has fueled a major research effort to design selective inhibitors of these proteases. Interestingly, γ-secretase cleaves several proteins including Notch, E-cadherin, CD44 and ErbB-4 (erythroblastic leukemia viral oncogene homolog 4), which are important modulators of angiogenesis. The β-amyloid precursor protein, which is cleaved by β-secretase and γ-secretase to produce β-amyloid, is highly expressed in the endothelium of neoforming vessels suggesting that it might play a role during angiogenesis. These data prompted us to explore the effects of β and γ-secretase inhibitors of different structures on angiogenesis and tumor growth. Both the γ and β-secretase inhibitors tested reduce endothelial cell proliferation without inducing cellular toxicity, suppress the formation of capillary structures in vitro and oppose the sprouting of microvessel outgrowths in the rat aortic ring model of angiogenesis. Moreover, they potently inhibit the growth and vascularization of human glioblastoma and human lung adenocarcinoma tumors xenotransplanted into nude mice. Altogether these data suggest that the γ and β-secretases play an essential role during angiogenesis and that inhibitors of the β and γ-secretases may constitute new classes of anti-angiogenic and anti-tumoral compounds.

Keywords: Tumor growth; Angiogenesis; Secretase; Amyloid precursor protein; Presenilin

1. Introduction

The β-amyloid precursor protein is a large glycoprotein highly expressed in neurons but also in vascular cells including endothelial cells (Forloni et al., 1992). It is cleaved by γ-secretase and by β-secretase generating β-amyloid and carboxyl terminal intracellular fragments (Sinha and Lieberburg, 1999). Amyloid plaques (invariantly associated with Alzheimer's disease), as well as vascular amyloid deposits in cerebral amyloid angiopathy contain β-amyloid, which is believed to play a key role in Alzheimer's disease pathophysiology (Hardy and Selkoe, 2002). Therefore, selective inhibitors of β and γ-secretase have been developed as possible therapeutic agents for Alzheimer's disease (Vassar, 2002; Roberts, 2002).

The β-amyloid precursor protein is highly expressed very early during fetal life in the endothelia of neovascularized tissue and particularly in cerebral endothelia (Ott and Bullock, 2001), which could suggest a normal role for the β-amyloid precursor protein and/or its metabolites in early angiogenesis. In addition, mice lacking γ-secretase activity display abnormal blood vessel development and exhibit cerebral hemorrhages and subcutaneous edema (Nakajima et al., 2003). We therefore explored the effect of various β and γ-secretase inhibitors of different molecular structures on angiogenesis. Additionally, we determined the effect of β and γ-secretase inhibitors on the growth of human brain glioblastoma and lung adenocarcinoma xenografts into nude mice, which are dependent on angiogenesis for their growths.

* Corresponding author. Tel.: +1 941 752 2949; fax: +1 941 752 2948.
E-mail address: dparis@rfdn.org (D. Paris).

0014-2999/$ - see front matter © 2005 Elsevier B.V. All rights reserved.
doi:10.1016/j.ejphar.2005.02.050

2. Methods

2.1. Isolation and culture of endothelial cells from microvessel outgrowths

Endothelial cells were isolated from human middle cerebral arteries as previously described (Paris et al. 2004). Briefly, segments of human middle cerebral arteries collected following rapid autopsies (2 to 4 h post-mortem delay) were embedded in 500 μl of Matrigel (Becton-Dickinson, Bedford, MA) in 24 well plates and covered with endothelial basal medium (EBM, Cambrex Bio Science, MD) supplemented with 4% fetal bovine serum and 1× penicillin–streptomycin–fungizone mixture. Following 9 days in culture with the medium being changed every 3 days, Matrigel containing microvessel outgrowths from human middle cerebral arteries were dissected with the aid of an inverted microscope and dissociated several times in EBM through a sterile pipette tip. Matrigel fragments were then plated on plastic culture flasks, and incubated in EBM (supplemented with 4% fetal bovine serum and 1× penicillin–streptomycin–fungizone mixture) at 37 °C, 5% CO_2 with medium changed every 3 days. After 5 to 6 days in culture, cells were subjected to a double immunostaining with an antibody against factor VIII and an antibody against α-smooth muscle actin in order to verify their endothelial nature.

2.2. Measurement of human brain endothelial cells viability and proliferation

Primary cultures of human brain endothelial cells were plated at a density of 10^4 cells/200 μL of EBM containing 4% of fetal bovine serum in 96 wells culture plates and treated with various doses of β and γ-secretase inhibitors as indicated in the figure legends. Following 24 h in culture, the EBM covering the cells was removed and assayed for Lacticodehydrogenase (LDH) activity using the cytotoxicity detection kit (Roche Diagnostic Corporation, IN). Cells were covered with 100 μL of EBM supplemented with 4% fetal calf serum and cellular proliferation measured using the Quick cell proliferation assay kit (Biovision Research Products, CA).

2.3. Capillary morphogenesis assay

Two hundred microliters of Matrigel was placed into each well of a 24-well culture plate at 4 °C and allowed to polymerize by incubation at 37 °C. Human middle cerebral artery endothelial cells (5×10^4) were seeded on the Matrigel in 1 ml of EBM containing 4% fetal calf serum. The cells were incubated at 37 °C for 20 h in a humidified 5% CO_2 atmosphere in the presence or absence of various doses of β and γ-secretase inhibitors as indicated in the figure legends (peptidomimetic β-secretase inhibitors OM99-2 (Glu-Val-Asn-Leu-Ψ-Ala-Ala-Glu-Phe [Ψ denotes replacement of CONH by (*S*)-CH(OH)CH_2]) and P_{10}–$P_{4'}$ statV that are not cell permeable were treated with the Pro-ject™ protein transfection reagent kit (Pierce, IL) and control conditions were established using the same dose of Pro-ject™ protein transfection reagent alone using the manufacturer's recommendations). The experiments were performed in quadruplicate for each treatment condition. For each culture, 2 randomly chosen fields were photographed using a 4× objective. An experimenter unaware of the different treatments measured the total length of tube structures in each photograph using the Image Pro Plus software (Media Cybernetic, Inc., MD). Capillary network lengths for the different treatment conditions were expressed as the percentage of capillary network lengths obtained in the control condition.

2.4. α-sAPP immunoprecipitation, sodium dodecyl sulfate–polyacrylamid gel electrophoresis (SDS–PAGE) and immunoblotting

Confluent Human brain endothelial cells (grown on 75-cm^2 flasks with EBM containing 4% fetal bovine serum) were treated for 24 h with 5 μM of Z-VLL-CHO (*N*-Benzyloxycarbonyl-Val-Leu-leucinal), 5 μM of L-685,458 ({1*S*-benzyl-4*R*-[1-(1*S*-carbamoyl-2-phenylethylcarbamoyl)-1*S*-3-methyl-butylcarbamoyl]-2*R*-hydroxy-5-phenylpentyl}carbamic acid *tert*-butyl ester), 5 μM of OM99-2 (in presence of Pro-ject™ protein transfection reagent kit (Pierce, IL)), 5 μM of DAPT (*N*-[*N*-(3,5-Difluorophenacetyl-L-alanyl)]-*S*-phenylglycine *t*-Butyl Ester) or went untreated (control). Experiments were done in quadruplicate for each treatment condition. 6E10 (Signet), a monoclonal antibody (mAb) that recognizes residues 1–17 of human Aβ, was used to immunoprecipitate the soluble β-amyloid precursor protein (sAPPα) generated following cleavage by α-secretase from cell culture medium. Immunoprecipitated material was resolved on a 4–20% gradient SDS–PAGE, transferred to Polyvinylidene Fluoride membranes (PVDF) and immunodetected with mAb 22C11 (Roche Diagnostics) that recognizes the amino acids 66–81 of the N-terminal portion of the β-amyloid precursor protein. Human brain endothelial cells were lysed on ice using MPER reagent (Pierce, IL) supplemented with 1 mM phenyl methyl sulfonyl fluoride (PMSF) and 1 mM of sodium-orthovanadate. Samples were sonicated and centrifuged at 10 000×*g* for 30 min at 4 °C. The protein content of the lysates was determined using the BCA Protein assay kit (Pierce, IL). Total lysates (50 μg of protein/sample) were separated on a 4–20% gradient SDS–PAGE and transferred to PVDF membranes and immunoprobed with mAb 22C11 in order to detect full length β-amyloid precursor protein and also immunoprobed with an Anti-APP-CT20 (Calbiochem, CA) antibody which recognizes the amino acid residues 751–770 of the carboxyl terminal region of the β-amyloid precursor protein (Pinnix et al., 2001).

2.5. Arterial explant assay

Twenty-four well tissue culture grade plates (Nalgene International, NY) were covered with 250 μL of Matrigel (Becton-Dickinson, Bedford, MA) and allowed to gel for 30 min at 37 °C, 5% CO_2. Briefly, thoracic aortae were excised from 9-month-old Sprague–Dawley rats. After removing the fibroadipose tissue, arteries were sectioned into 1-mm-long cross-sections, rinsed 5 times with EBM (Clonetics, CA) containing 4% fetal bovine serum and placed on the Matrigel coated wells. Artery rings were covered with an additional 250 μL of Matrigel. After polymerization the Matrigel was covered with 1 ml of EBM (supplemented with 4% fetal bovine serum) containing various doses of Z-VLL-CHO, OM99-2, P_{10}–$P_{4'}$ statV (peptidomimetic β-secretase inhibitors OM99-2 and P_{10}–$P_{4'}$ statV that are not cell permeable were treated with the Pro-ject™ protein transfection reagent kit (Pierce, IL) and control conditions were established using the same dose of Pro-ject™ protein transfection reagent alone using the manufacturer's recommendations), DAPT, JLK-6 or L-685,458 as indicated in the

figure legends (the culture medium was changed every 3 days). Pictures were taken at days 4, 5 and 6 using a 4× objective. Microvessel outgrowth area was quantified using the Image Pro Plus software. Briefly, ring cultures were photographed using a digital video camera linked to an Olympus BX60 microscope. The outgrowth area was delineated and measured with the Image Pro Plus software by using a strategy of microvessel outgrowth detection based on difference in color intensities between the outgrowths, the Matrigel and the artery ring. The artery rings were manually selected and excluded from the area of measurement and the color intensity threshold was adjusted to selectively measure the area occupied by the microvessel outgrowths. Results were expressed as a percentage of the area occupied by microvessel outgrowths at day 4 in control condition.

2.6. Tumor xenograft models

The human glioblastoma U-87 MG and human lung adenocarcinoma A-549 cell lines were obtained from American Tissue Culture Type Collection (Manassas, VA) and were grown in Dulbecco's Modified Eagle Medium (DMEM) containing 1× penicillin–streptomycin–fungizone and 10% fetal bovine serum at 37 °C in a humidified atmosphere of 5% CO_2. Tumor cells (6×10^6) in 100 μl of PBS (Phosphate Buffered Saline) were inoculated subcutaneously into both flanks of 8–10-week-old female nude mice (Harland Teklad, WI). Tumor volume (in mm^3) was determined using the formula (length × $width^2$)/2, where length was the longest axis and width the measurement at right angles to the length (Clarke et al., 2000). When the tumor volumes reached approximately 150 mm^3,

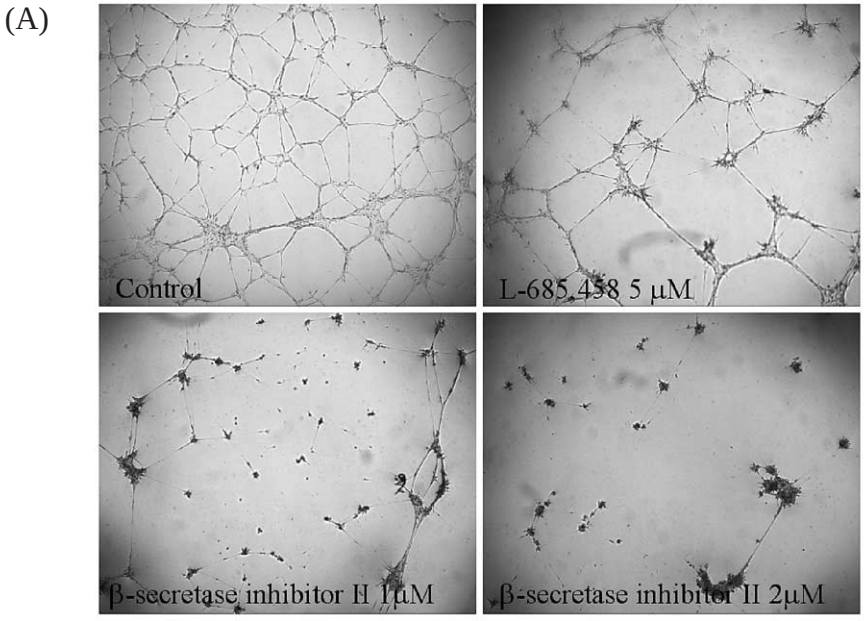

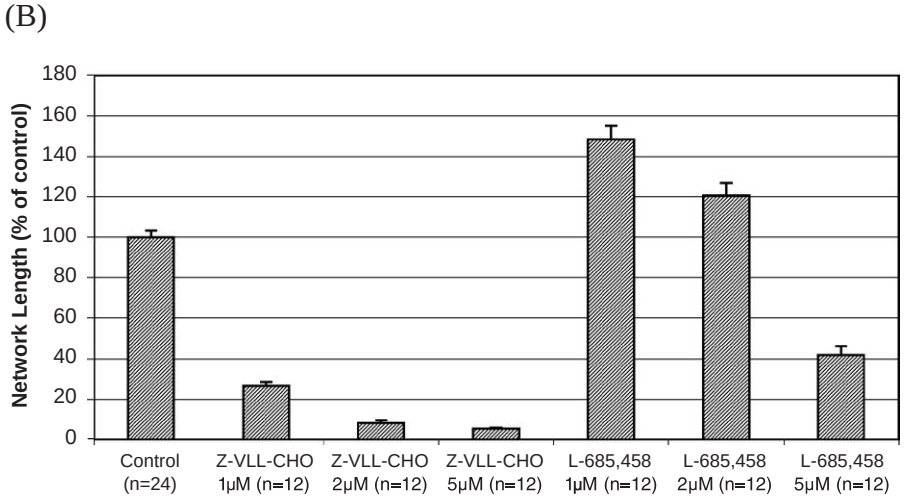

Fig. 1. (A) Representative pictures showing the effect of L-685,458 and Z-VLL-CHO (β-secretase inhibitor II) on capillary morphogenesis induced by plating human brain endothelial cells on Matrigel reconstituted basement membrane. (B) Quantification of network length by Image analysis. The numbers in parenthesis on the *x*-axis represent the number of 4× fields analyzed. ANOVA revealed significant main effects of Z-VLL-CHO ($P < 0.001$) and L-685458. Post-hoc testing showed significant difference between control and Z-VLL-CHO for all the doses tested ($P < 0.001$) and between control and L-685458 for all the doses tested ($P < 0.001$).

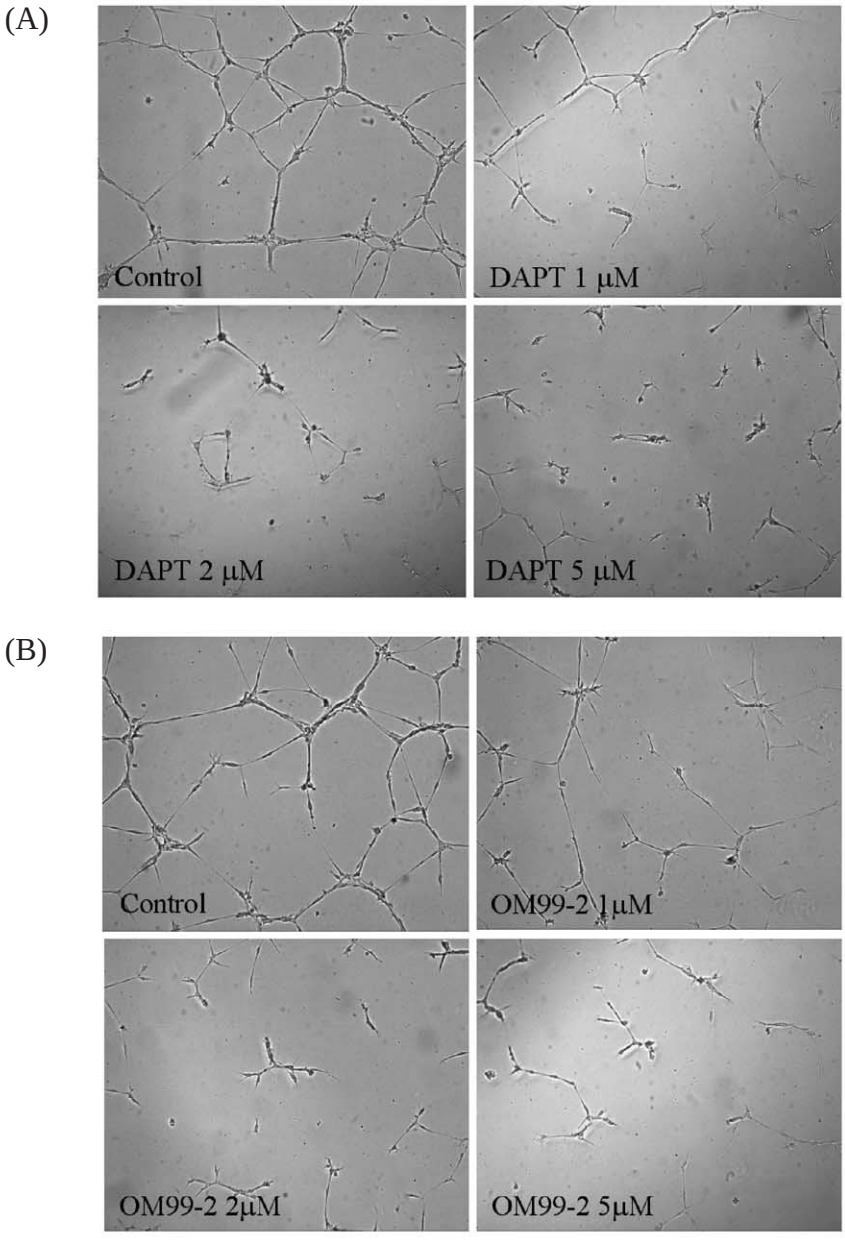
(A)
Control
DAPT 1 μM
DAPT 2 μM
DAPT 5 μM
(B)
Control
OM99-2 1μM
OM99-2 2μM
OM99-2 5μM
(C)
Network Length (% of control)
120
100
80
60
40
20
0
Control (n=8)
DAPT 1μM (n=8)
DAPT 5μM (n=8)
OM99-2 100nM (n=8)
OM99-2 1μM (n=8)
OM99-2 2μM (n=8)
OM99-2 5μM (n=8)

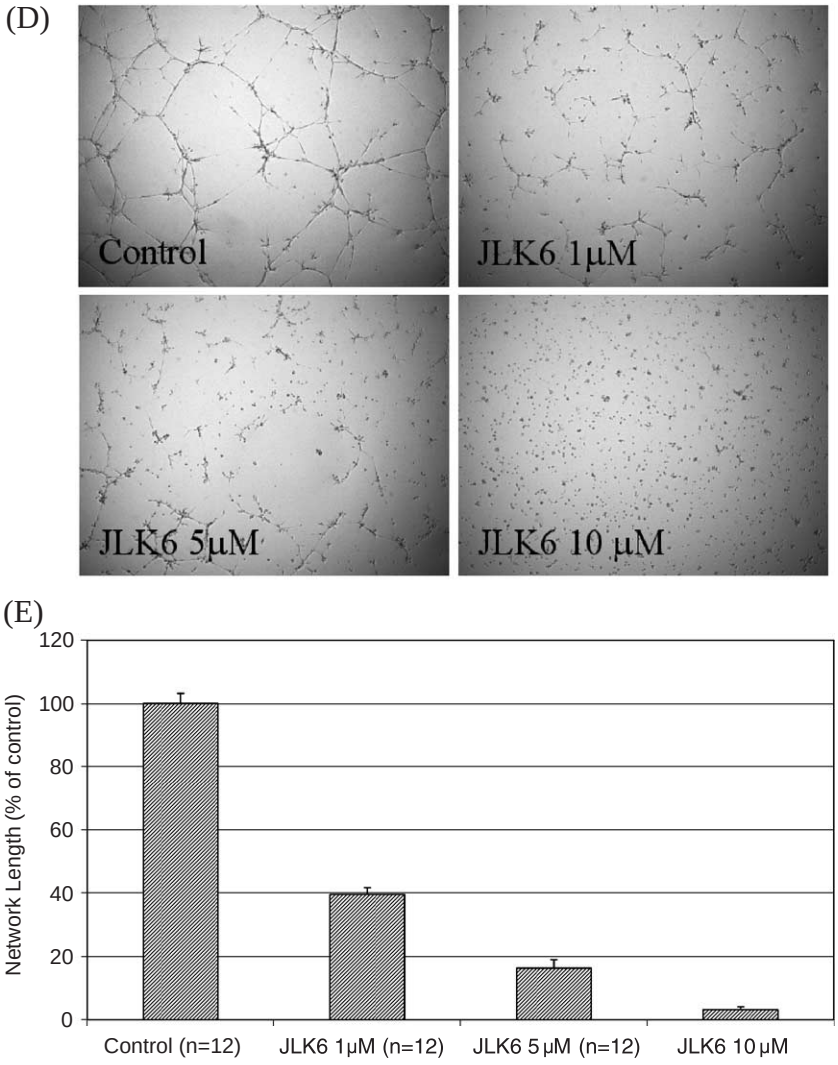

Fig. 2. Representative pictures showing the effect of (A) various DAPT doses, of (B) various OM99-2 doses and (D) various JLK6 doses on capillary morphogenesis induced by plating human brain endothelial cells on Matrigel reconstituted basement membrane. (C) Quantification of network length by Image analysis following DAPT and OM99-2 treatments. The numbers in parenthesis on the *x*-axis represent the number of 4× fields analyzed. ANOVA revealed significant main effects of DAPT dose and OM99-2 dose ($P<0.001$). Post-hoc testing showed significant difference between control and DAPT 1 μM ($P<0.005$), control and OM99-2 1 μM ($P<0.005$), control and DAPT 5 μM ($P<0.001$), control and OM99-2 2 μM ($P<0.001$) and between control and OM99-2 5 μM ($P<0.001$). (E) Quantification of network length by Image analysis following JLK6 treatment. The numbers in parenthesis on the *x*-axis represent the number of 4× fields analyzed. ANOVA revealed significant main effect of JLK6 dose ($P<0.001$) and post-hoc comparison showed significant difference between control and JLK6 1 μM ($P<0.001$), control and JLK6 5 μM ($P<0.001$) and between control and JLK6 10 μM ($P<0.001$).

animals were treated intraperitoneally everyday with 100 μl of 50% Dimethyl Sulfoxide/H_2O (vehicle group), 5 mg/kg of body weight of Z-VLL-CHO (β-secretase inhibitor), 5 mg/kg of JLK-6 (γ-secretase inhibitor) or with 10 mg/kg of body weight of DAPT. Data were expressed as mean tumor volume ± S.E for each treatment group. At the completion of the study, animals were humanely euthanatized and tumors were harvested and fixed in paraformaldehyde 4% overnight at 4 °C. After paraffin embedding in an automated tissue processing Sakura Tissue-Tek (E150) (Torrence, CA), samples were cut into 5-μm sections, deparafinized, and rehydrated through a graded series of alcohol. Sections were treated with 0.02 mg/ml Proteinase K (Gentra Systems, MN) for 15 min at 37 °C to allow for proper antigen retrieval, washed several times in PBS and incubated for 15 min in a 0.3% solution of hydrogen peroxide. Sections were blocked and then immunostained with a 1:40 dilution of a PECAM-1 (Platelet Endothelial Cell Adhesion Molecule) antibody (BD-Pharmingen, CA) overnight at 4 °C in a humidification chamber. Vector ABC Kits (Vector Laboratories Inc., CA) were used following the manufacturer's instruction for the immunostaining. Quantification of tumor vascularization was performed using the stereological dissector method (Artacho-Perula and Roldan-Villalobos, 1995; Braendgaard and Gundersen., 1986). Briefly, 40 consecutive sections were taken from a randomly chosen starting point in each tumor. Five sections for each tumor were selected for stereology by taking one section every eight sections. A dissector counting frame was used with inclusion and exclusion lines throughout the reference area made of 12 squares of 0.0012 mm^2. Vessel count was performed at ×400 magnification with the use of an Olympus BX60 microscope connected to a digital video camera. Microvessels were counted in the dissector frame by an experi-

menter unaware of the different treatment conditions. For each tumor the length of vessels in the dissector frame (Lv) was estimated using the following formulae: Lv=(2 × average vessel count)/ reference area. The total length of vessels for each tumor was estimated by multiplying Lv by the tumor volume. A vascular index was calculated by expressing the vessel length as a percentage of the vessel length in the vehicle treatment condition.

2.7. Statistical analysis

Multiple comparisons were evaluated by analysis of variance and post hoc comparisons performed with Bonferroni's method using SPSS V12.0.1 for Windows. Probability values less than 5% were considered statistically significant.

3. Results

3.1. Effect of β and γ-secretase inhibitors on capillary morphogenesis

Angiogenesis, the growth of new capillaries from preexisting vessels, is a tightly regulated process which requires specific steps including: (a) the release of proteases from "activated" endothelial

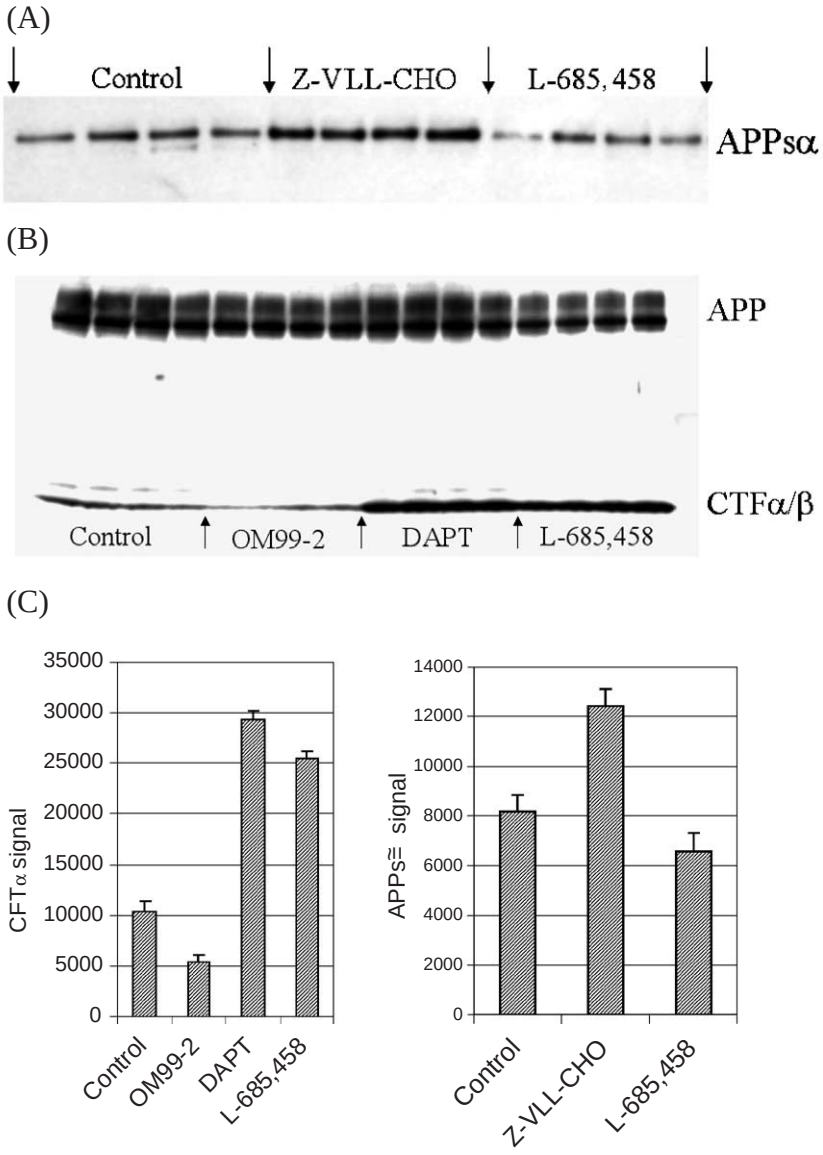

Fig. 3. Effects of β and γ-secretase inhibitors on the metabolism of APP in human brain endothelial cells. (A) Culture media were analyzed by immunoblotting to measure the secretion of α-secretase cleaved amyloid precursor protein (α-sAPP) molecules. (B) Carboxyl-terminal amyloid precursor protein fragments and full length amyloid precursor protein (APP) from human brain endothelial cell lysates. (C) Quantification of α-sAPP molecules secreted in the culture media of human brain endothelial cells. ANOVA revealed a significant main effect for Z-VLL-CHO ($P<0.003$) but not for L-685 458 ($P=0.13$) and post-hoc analysis showed significant differences between control and Z-VLL-CHO ($P<0.006$) showing that Z-VLL-CHO significantly increased the secretion of α-sAPP. Quantification of carboxyl-terminal amyloid precursor protein fragments generated by human brain endothelial cells. ANOVA revealed significant main effects of OM99-2 ($P<0.002$), L-685458 ($P<0.001$) and DAPT ($P<0.001$). Post-hoc testing showed significant differences between control and OM99-2 ($P<0.009$), control and DAPT ($P<0.001$) and between control and L-685458 ($P<0.001$) showing that DAPT and L-685458 stimulates whereas OM99-2 significantly reduces the accumulation of carboxyl-terminal amyloid precursor protein fragments.

cells resulting in degradation of the basement membrane surrounding the existing vessel; (b) migration of endothelial cells into the interstitial space; (c) endothelial cell proliferation, and (d) differentiation into mature blood vessels (Carmeliet, 2000). In order to determine the possible contribution of β and γ-secretase to the angiogenic process, we used several selective β and γ-secretase inhibitors of unrelated structures in in vitro and ex vivo models of angiogenesis. We first investigated the effect of L-685,458 ({1*S*-benzyl-4*R*-[1-(1*S*-carbamoyl-2-phenylethylcarbamoyl)-1*S*-3-methyl-butylcarbamoyl]-2*R*-hydroxy-5-phenylpentyl}carbamic acid *tert*-butyl ester) an aspartyl protease transition-state inhibitor of γ-secretase (Shearman et al., 2000) on the proliferation of primary cultures of human brain endothelial cells. We observed that L-685,458 dose dependently (1 to 5 μM) inhibits the proliferation of human brain endothelial cells without inducing cellular toxicity (data not shown). We next investigated the effect of L-685,458 on the formation of capillary networks. When plated on a reconstituted basement membrane (Matrigel), endothelial cells differentiate into a network of capillary structures. The Matrigel matrix, like the in vivo basement membrane, furnishes a rich environment to promote angiogenesis. Electron microscopy has demonstrated that the tubular structures formed by endothelial cells in this model are vascular-like structures containing lumens (Kubota et al., 1988). L-685,485 dose dependently inhibited capillary morphogenesis (Fig. 1). We next tested the effects of the previously described functional γ-secretase inhibitor DAPT (*N*-[*N*-(3,5-Difluorophenacetyl-L-alanyl)]-*S*-phenylglycine *t*-Butyl Ester) (Dovey et al., 2001; Sastre et al., 2001). Similarly to L-685,485, DAPT dose dependently inhibited the proliferation (data not shown) and the differentiation of primary cultures of human brain endothelial cells into capillaries (Fig. 2). In addition, similar data were obtained with the γ-secretase inhibitor DAPM (data not shown). The different γ-secretase inhibitors that we used are also known to affect Notch cleavage therefore we also tested JLK6 (7-Amino-4-chloro-3-methoxyisocoumarin), a compound which has been shown to inhibit the cleavage of APP by γ-secretase without affecting the Notch pathway (Petit et al., 2001). Interestingly, JLK6 also inhibited capillary morphogenesis in a dose-dependent manner (Fig. 2).

To determine whether β-secretase activity was required during angiogenesis, we investigated the effect of different β-secretase

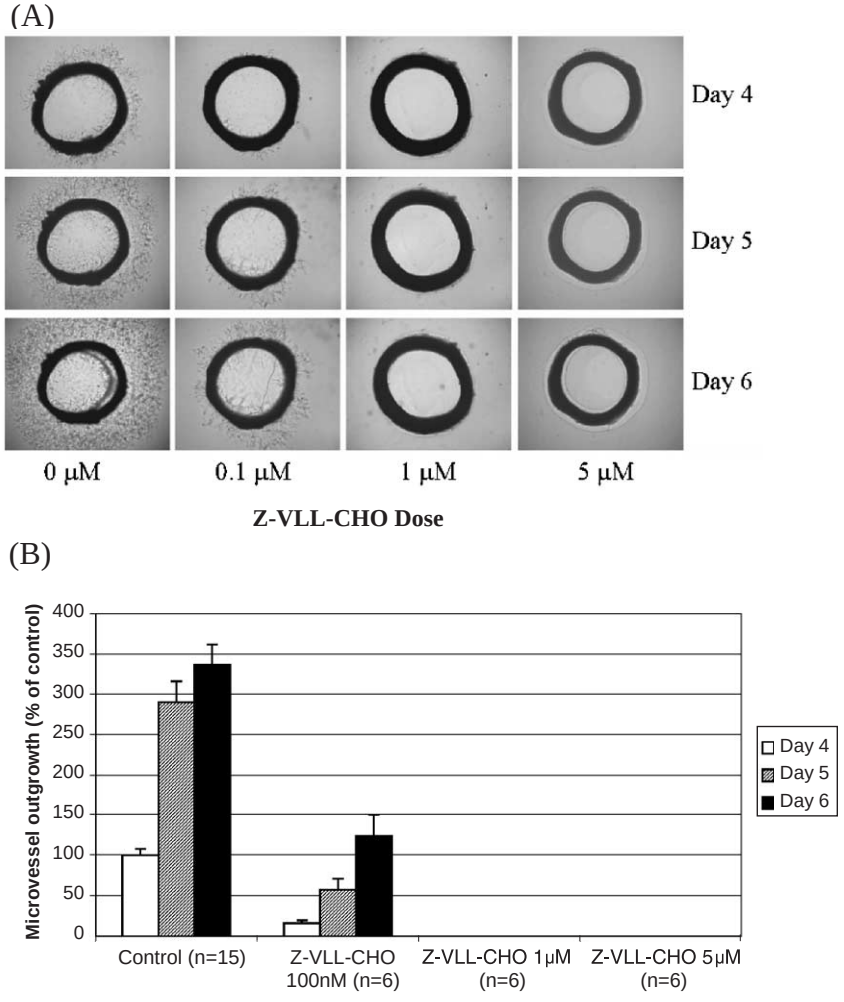

Fig. 4. The β-secretase inhibitor Z-VLL-CHO dose-dependently inhibits the formation of microvessel outgrowths by explants of rat aortae. (A) Representative pictures of rat aortic rings embedded in Matrigel showing the progressive sprouting of capillaries with time in function of the dose of Z-VLL-CHO used. (B) Quantification by image analysis of the area covered by microvessel outgrowths. ANOVA revealed a significant main effect of Z-VLL-CHO dose ($P<0.001$) and time ($P<0.001$) as well as an interactive term between them ($P<0.001$). Post-hoc testing showed significant differences between control and 100 nM Z-VLL-CHO ($P<0.001$), control and 1 μM Z-VLL-CHO ($P<0.001$) and between control and 5 μM Z-VLL-CHO ($P<0.001$).

inhibitors on endothelial cell proliferation and capillary morphogenesis. We first used the β-secretase inhibitor II (Z-VLL-CHO; *N*-Benzyloxycarbonyl-Val-Leu-leucinal), a simple tripeptide aldehyde designed from the β-secretase cleavage site (VNL-DA) which shows inhibition of β-secretase activity at low μM concentrations (Abbenante et al., 2000). Z-VLL-CHO dose dependently inhibited the proliferation of human brain endothelial cells without affecting their viability (data not shown). In addition, this compound potently and dose dependently inhibited the formation of capillary structures in the capillary morphogenesis assay (Fig. 1). To further confirm the involvement of β-secretase in angiogenesis, we tested the effect of OM99-2 (Glu-Val-Asn-Leu-Ψ-Ala-Ala-Glu-Phe [Ψ denotes replacement of CONH by (*S*)-$CH(OH)CH_2$]), a peptidomimetic tight binding transition-state analog inhibitor of β-secretase (Hong et al., 2000). OM99-2 dose dependently inhibited endothelial cell proliferation (data not shown) and angiogenesis in the capillary morphogenesis assay (Fig. 2). Similar data were also obtained with the β-secretase inhibitor GL189 (data not shown).

In order to verify the functionality of the β and γ-secretase inhibitors used on endothelial cells, we determined the effects of these compounds on the processing of APP by human brain endothelial cells. We observed that the β-secretase inhibitor II (Z-VLL-CHO) stimulated the secretion of the α-secretase cleaved amyloid precursor protein fragment (α-sAPP) suggesting inhibition of β-secretase activity. The γ secretase inhibitors DAPT and L-685,485 promoted the accumulation of the amyloid precursor protein intracellular terminal fragments (CTF) in human brain endothelial cells modeling the accumulation of APP CTF habitually observed in PS1 knockout cells deficient in γ-secretase activity (Fig. 3).

3.2. Effect of β and γ-secretase inhibitors on the sprouting of microvessels from explants of rat aortae

To further study the effect of the β-secretase and γ-secretase inhibitors on angiogenesis, we used the rat aortae model of angiogenesis, which has been shown to correlate well with in vivo events of neovascularization. In this assay, angiogenesis is a self-

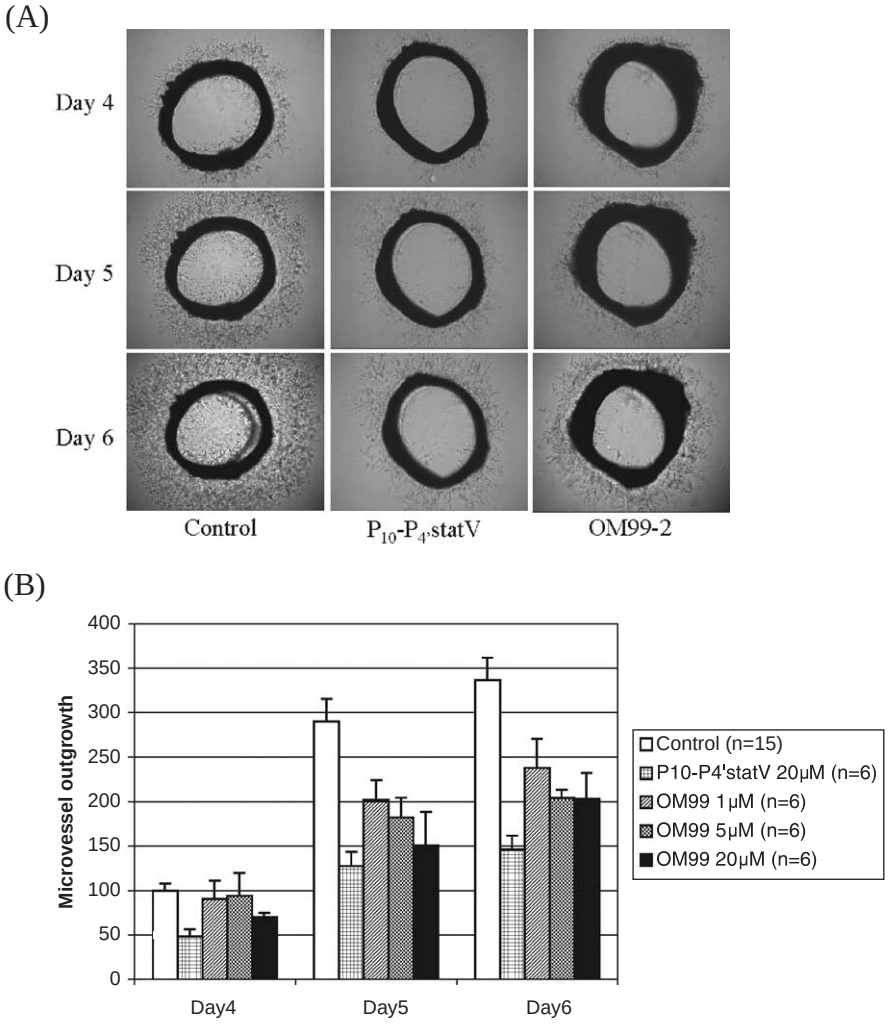

Fig. 5. Effect of the β-secretase inhibitors OM99-2 and $P_{10}-P_{4'}$ statV on the sprouting of microvessels by explants of rat aortae. (A) Representative pictures showing the formation of microvessel outgrowths in function of time for control aortic rings, for aortic rings treated with 20 μM of $P_{10}-P_{4'}$ statV and aortic rings treated with 20 μM of OM99-2. (B) Quantification by image analysis of the area covered by microvessel outgrowths. ANOVA revealed significant main effects for $P_{10}-P_{4'}$ statV ($P<0.001$) and for OM99-2 dose ($P<0.001$) as well as an interactive term between time and $P_{10}-P_{4'}$ statV ($P<0.002$) and between time and OM99-2 dose ($P<0.002$). Post-hoc testing across day 5 and day 6 showed significant differences between control and $P_{10}-P_{4'}$ statV ($P<0.001$), control and 1 μM OM99-2 ($P<0.003$), control and 5 μM OM99-2 ($P<0.001$) and between control and 20 μM OM99-2 ($P<0.001$).

limited process, triggered by injury and regulated by well-defined autocrine/paracrine mechanisms (Nicosia et al., 1997). In this model, the rat aortic endothelium exposed to a three-dimensional matrix switches to a microvascular phenotype generating branching networks of microvessels (Nicosia et al., 1992). We observed that the β-secretase inhibitor Z-VLL-CHO dose dependently and potently inhibited the sprouting of microvessels from explants of rat aortae (Fig. 4). The β-secretase inhibitors OM99-2 and $P_{10}-P_{4'}$ statV (a substrate analogue peptide inhibitor of β-secretase which has been used to purify β-secretase from human brain (Sinha and Lieberburg, 1999) also suppressed the formation of microvessel outgrowths from explants of rat aortae (Fig. 5). The functional γ-secretase inhibitor DAPT was also tested in this rat aortic ring model of angiogenesis and appeared to dose dependently inhibit

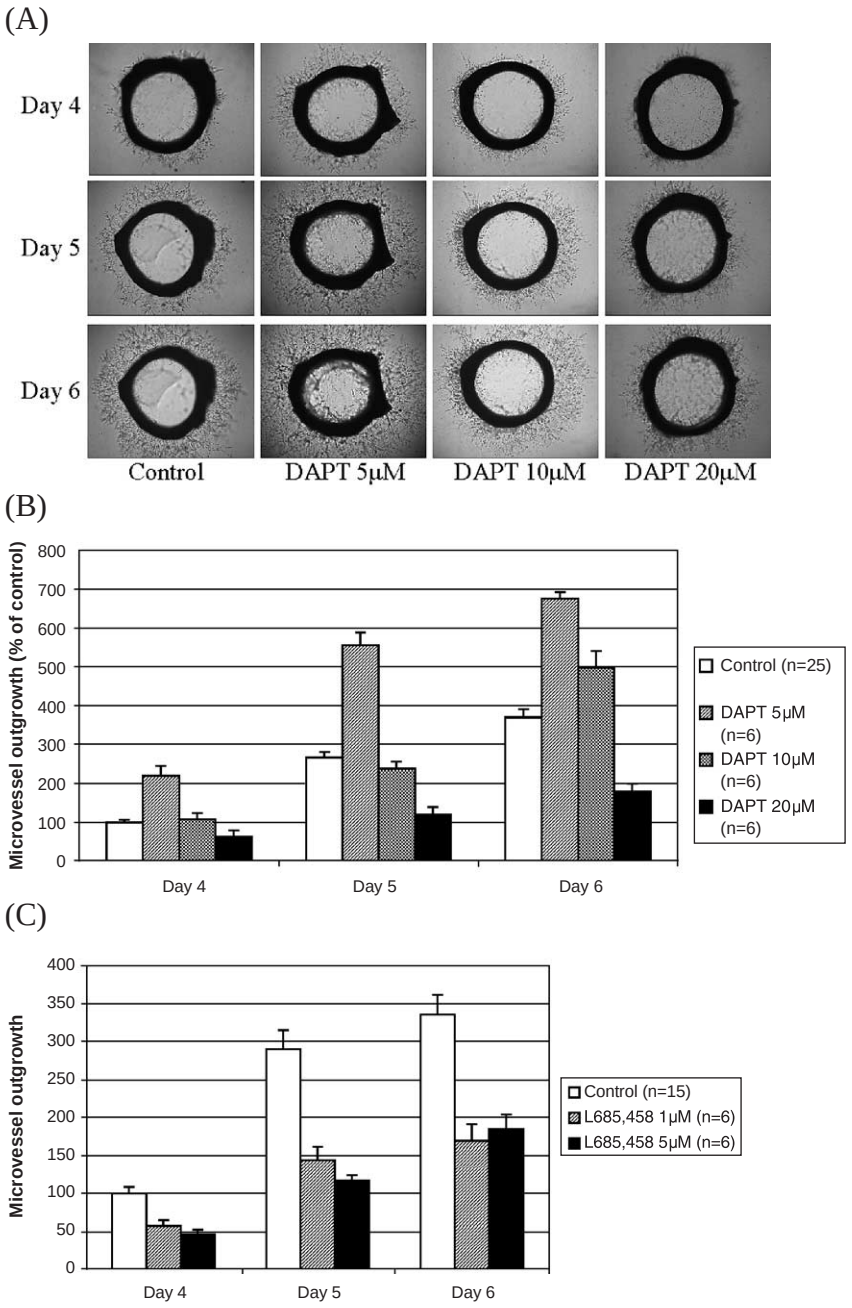

Fig. 6. Effects of γ-secretase inhibitors on the formation of microvessel outgrowths by explants of rat aortae. (A) Representative pictures depicting the effect of DAPT on microvessel outgrowths. (B) Quantification by image analysis of the area covered by microvessel outgrowths following DAPT treatment. ANOVA revealed significant main effects of DAPT dose ($P<0.001$) and time ($P<0.001$) as well as an interactive term between them ($P<0.001$). Post-hoc testing showed significant differences between control and DAPT 5 μM ($P<0.001$), between control and DAPT 20 μM ($P<0.02$) but no significant difference between control and DAPT 10 μM ($P=0.999$). (C) Quantification by image analysis of the area covered by microvessel outgrowths following L-685,458 treatment. ANOVA revealed significant main effects of L-685,458 ($P<0.001$) and time ($P<0.001$) as well as an interactive term between them ($P<0.005$). Post-hoc testing showed significant differences between control and 1 μM L-685,458 ($P<0.002$) and between control and 5 μM L-685,458 ($P<0.001$).

the sprouting of new capillaries (Fig. 6). Similar data were also obtained with the γ-secretase inhibitor L-685,458 (Fig. 6).

3.3. Effect of β-secretase inhibitor and of the γ-secretase inhibitors on the growth of tumor xenografts in nude mice

Tumor growth is generally dependent on angiogenesis. This is particularly true for brain tumors such as glioblastoma, which are highly vascularized tumors. We therefore investigated the effect of the γ-secretase inhibitor DAPT and of the β-secretase inhibitor Z-VLL-CHO on the growth of human glioblastoma and human lung adenocarcinoma xenografted under the skin of nude mice. We observed that both the β and γ-secretase inhibitors used potently inhibited the growth of U87MG brain tumors (Fig. 7). Vascularization of the tumors was evaluated by PECAM-1 immunostaining. A decreased vascularization was observed in U87MG tumors

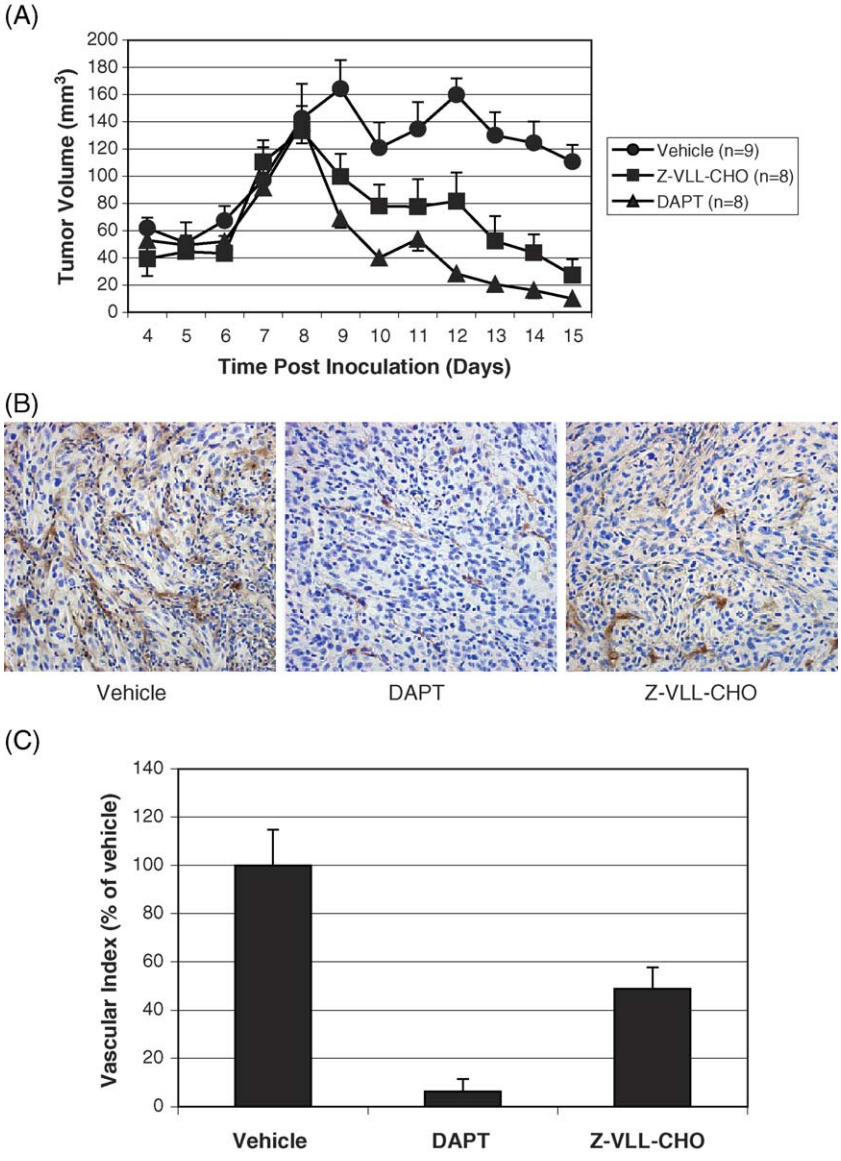

Fig. 7. (A) Anti-tumoral effect of the γ-secretase inhibitor DAPT and of the β-secretase inhibitor Z-VLL-CHO on human glioblastoma (U-87 MG) xenografts growth rates. U-87 MG cells (6×10^6) were injected subcutaneously into both flanks of 8–10-week-old nude mice. Mice were injected intraperitoneally with either the vehicle (●), 5 mg/kg of body weight of the β-secretase inhibitor Z-VLL-CHO (■) or 10 mg/kg of body weight of the γ-secretase inhibitor DAPT (▲) starting when tumors had reached a mean tumor volume of approximately 140 mm^3 (day 8 post-implantation). Injections were given everyday for 9 days. Data are expressed as mean tumor volume±S.E. ANOVA reveals significant main effect of DAPT ($P<0.001$) and Z-VLL-CHO ($P<0.001$) and time ($P<0.001$). Post-hoc analysis shows significant differences between the tumor volumes from vehicle treated mice and DAPT treated animals ($P<0.001$), from vehicle treated mice and Z-VLL-CHO treated mice ($P<0.001$) but no difference between Z-VLL-CHO and DAPT treatments ($P=0.12$) showing that Z-VLL-CHO and DAPT inhibit the growth of human glioblastoma xenografts with a similar potency. (B) Representative pictures of sections of glioblastoma tumors immunostained with CD31 antibodies. (C) Histogram depicting the estimation of glioblastoma tumor vascularization. ANOVA reveals significant main effects of DAPT ($P<0.001$) and Z-VLL-CHO ($P<0.02$). Post-hoc analysis shows significant differences between the vascular index of vehicle treated mice and DAPT treated mice ($P<0.002$) and between the vascular index of vehicle treated mice and Z-VLL-CHO treated animals ($P<0.03$) showing that Z-VLL-CHO and DAPT significantly reduce the vascularization of human glioblastoma xenografts.

treated with DAPT and Z-VLL-CHO compared with the vehicle treatment group suggesting that both DAPT and Z-VLL-CHO are able to inhibit tumor angiogenesis in vivo. We also tested the effect of DAPT and Z-VLL-CHO on the proliferation of U87MG tumor cells and observed that the β-secretase inhibitor Z-VLL-CHO and the γ-secretase inhibitor DAPT dose dependently inhibit the proliferation of these tumor cells without inducing tumor cell death (data not shown). Similar data were also obtained with the human lung adenocarcinoma cell line A549 (data not shown). We next tested the effect of DAPT and Z-VLL-CHO on the growth of

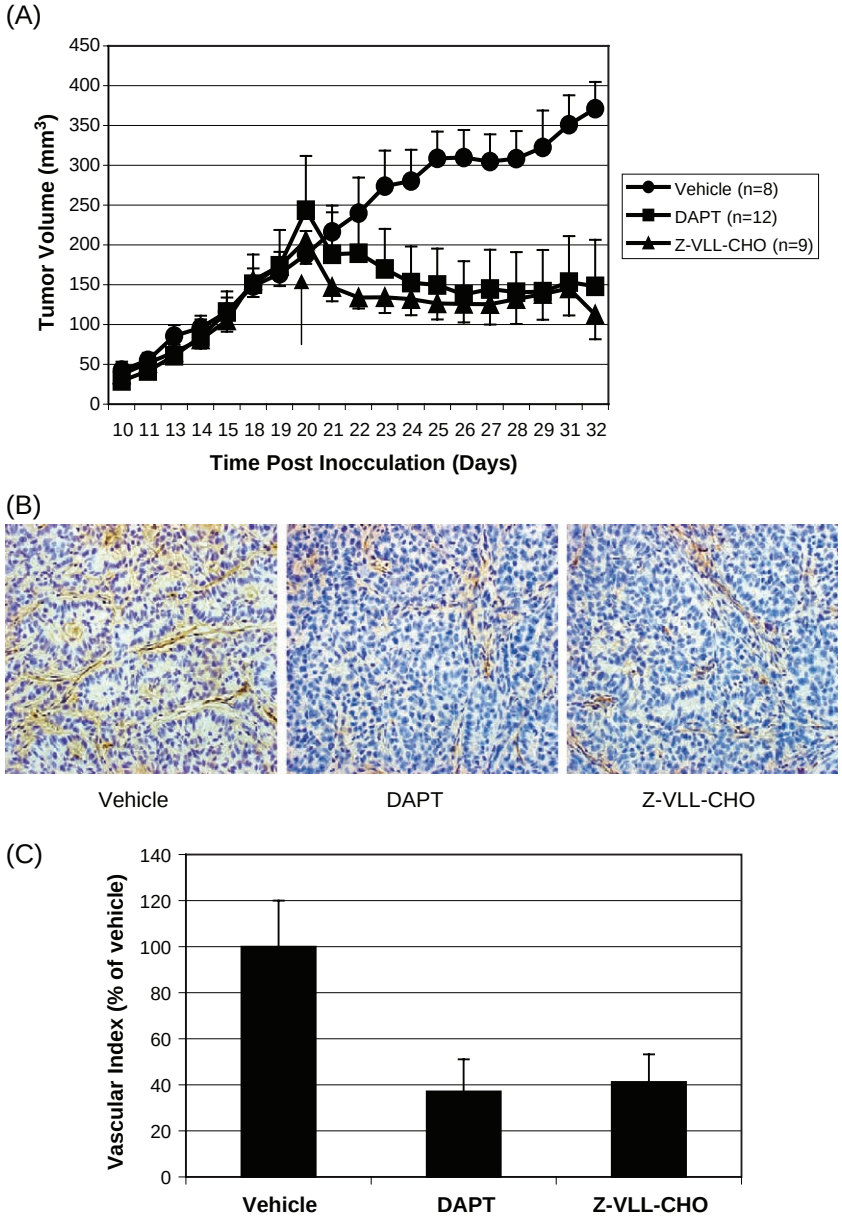

Fig. 8. (A) Anti-tumoral effect of the γ-secretase inhibitor DAPT and of the β-secretase inhibitor Z-VLL-CHO on human lung adenocarcinoma (A-549) xenografts growth rates. A-549 cells (8.5×10^6) were injected subcutaneously into both flanks of 8–10-week-old nude mice. Mice were injected intraperitoneally with either the vehicle (●), 5 mg/kg of body weight of the β-secretase inhibitor Z-VLL-CHO (■) or 10 mg/kg of body weight of the γ-secretase inhibitor DAPT (▲) starting when tumors had reached a mean tumor volume of approximately 200 mm^3 (day 21 post-implantation). Injections were given everyday for 12 days. Data are expressed as mean tumor volume±S.E. ANOVA reveals significant main effects of DAPT ($P<0.001$), Z-VLL-CHO ($P<0.001$) and time ($P<0.001$). Post-hoc analysis shows significant differences between the tumor volumes from vehicle treated mice and DAPT treated animals ($P<0.001$), from vehicle treated mice and Z-VLL-CHO treated mice ($P<0.001$) but no difference between Z-VLL-CHO and DAPT treatments ($P=0.519$) showing that DAPT and Z-VLL-CHO significantly inhibit the growth of human lung adenocarcinoma xenografts. (B) Representative pictures of sections of lung adenocarcinoma tumors immunostained with CD31 antibodies. (C) Histogram depicting the quantification of the vascularization of lung adenocarcinoma tumors. ANOVA reveals significant main effects of DAPT ($P<0.01$) and Z-VLL-CHO ($P<0.01$). Post-hoc analysis shows significant differences between the vascular index of vehicle treated mice and DAPT treated mice ($P<0.03$) and between the vascular index of vehicle treated mice and Z-VLL-CHO treated animals ($P<0.03$) showing that Z-VLL-CHO and DAPT significantly reduce the vascularization of human lung adenocarcinoma xenografts.

human lung adenocarcinoma tumors. Both compounds appear to potently suppress the growth of A549 lung adenocarcinoma tumors in nude mice (Fig. 8). In addition, the vascularization of A549 tumors appears to be decreased following DAPT or Z-VLL-CHO treatment suggesting in vivo inhibition of angiogenesis by DAPT and Z-VLL-CHO. We also tested the effect of JLK-6, a compound that has been shown to inhibit Aβ production without affecting Notch cleavage and observed that JLK-6 potently inhibits the growth and vascularization of human lung adenocarcinoma tumors xenotransplanted into nude mice (Fig. 9).

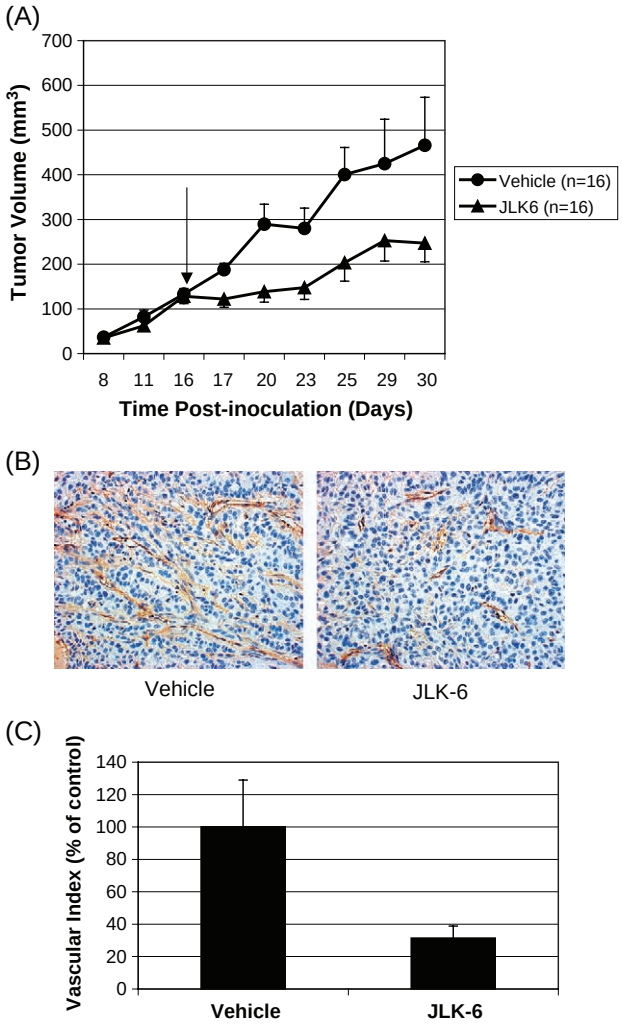

Fig. 9. (A) Anti-tumoral effect of the γ-secretase inhibitor JLK-6 on human lung adenocarcinoma (A-549) xenografts growth rates. A-549 cells (8.5×10^6) were injected subcutaneously into both flanks of 8–10-weeks-old nude mice. Mice were injected intraperitoneally everyday from Day 16 (when the tumors reached a volume of approximately 150 mm^3) with either the vehicle (●) or 5 mg/Kg of body weight of the γ-secretase inhibitor JLK-6 (▼). Data are expressed as mean tumor volume (mm^3)±S.E. ANOVA reveals significant main effects of JLK-6 ($P<0.001$) and time ($P<0.001$) showing inhibition of tumor growth in the JLK-6 treated group of animals compared to animals treated with the vehicle showing that JLK-6 significantly inhibits the growth of human lung adenocarcinoma xenografts. (B) Representative pictures of sections of lung adenocarcinoma tumors immunostained with CD31 antibodies. (C) Histogram depicting the quantification of the vascularization of lung adenocarcinoma tumors treated with the vehicle and with JLK-6. Significant mean differences were observed by *t*-test between vehicle treated and JLK-6 treated tumors ($P<0.04$) showing that JLK-6 significantly reduces the vascularization of human lung adenocarcinoma tumors.

4. Discussion

The involvement of β-secretase and γ-secretase in producing the β-amyloid component of plaques found in the brains of Alzheimer's patients has led to the design of selective inhibitors of these proteases that might be of therapeutic interest for Alzheimer's disease. The use of selective β and γ-secretase inhibitors might also be important to reveal cryptic functions of these proteases during other physiological processes opening the possibility of new applications for these drugs.

β-Secretase (also called BACE-1 for β-site amyloid precursor protein-cleaving enzyme) was identified as a type 1 transmembrane protein containing aspartyl protease activity (Vassar et al., 1999). BACE-1 mediates the primary amyloidogenic cleavage of the β-amyloid precursor protein and generates a membrane-bound amyloid precursor protein C-terminal fragment (APP CTFβ), which is the immediate precursor for the intramembranous γ-secretase cleavage. The γ-secretase which is a multiprotein high-molecular-weight complex formed by the association of presenilin 1, presenilin 2, APH-1 (anterior pharynx-defective phenotype), nicastrin and PEN-2 (presenilin-enhancer), ensures the cleavage of the β-amyloid precursor protein and also mediates the cleavage of several type-I integral membrane proteins, including the Notch receptor (De Strooper et al., 1999), E-cadherin, N-cadherin (Marambaud et al., 2002), CD44 (Murakami et al., 2003; Lammich et al., 2002), ErbB-4 (Ni et al., 2001), Nectin-1-alpha (Kim et al., 2002), the Notch ligands Delta and Jagged (Lavoie and Selkoe, 2003) and the low density lipoprotein (LDL) receptor-related protein (LRP) (May et al., 2002). Notch is a signaling molecule that regulates cell-fate determination during development (Pourquie, 2003). Signaling through Notch is triggered by the binding of ligands such as Delta and Jagged, which induces cleavage of Notch by TACE (Brou et al., 2000). Subsequent cleavage by γ-secretase releases the Notch intracellular domain, which binds to transcription factors and regulates transcription of *Enhancer of Split* complex genes (Greenwald., 1998). The processing of Notch and β-amyloid precursor protein shares striking similarities suggesting that they may have common functions: the cleavage of β-amyloid precursor protein by γ-secretase liberates a fragment analogous to the Notch intracellular domain, the amyloid precursor protein intracellular domain (AICD), which could regulate gene expression (Cao and Sudhof, 2001). Recently, AICD has been shown to regulate phosphoinositide-mediated calcium signaling through a γ-secretase dependent signaling pathway, suggesting that the intramembranous proteolysis of β-amyloid precursor protein may play a signaling role similar to that of Notch (Leissring et al., 2002). Notch signaling has

been implicated as a regulatory feature of the angiogenic process (Zhong et al., 2001; Mailhos et al., 2001; Zimrin et al., 1996). Other substrates of γ-secretase including Notch, CD44, E-cadherin, Delta, Jagged and ErbB-4 are also known to play a role during angiogenesis (Savani et al., 2001; Corada et al., 2002; Yen et al., 2002).

Vascular cells including smooth muscle cells and endothelial cells express the β-amyloid precursor protein as well as β and γ-secretase activities leading to the production of Aβ peptides (Simons et al., 1998). Interestingly, the β-amyloid precursor protein is expressed very early during fetal life in the endothelia of neovascularized tissue and particularly in cerebral endothelia (Ott and Bullock, 2001), which could suggest a normal role for the β-amyloid precursor protein and/or its metabolites in early angiogenesis. Mice lacking γ-secretase activity suffer from abnormal vessel formation (Nakajima et al., 2003; Herreman et al., 1999; Shen et al., 1997). In addition, γ-secretase is required for the processing of several proteins, which are known to play a role in angiogenesis. We therefore investigated the effect of various β and γ-secretase inhibitors of different molecular structures on angiogenesis using in vitro, ex vivo and in vivo models. We show that β and γ-secretase inhibitors are able to dose dependently affect the proliferation and the differentiation of human brain endothelial cells into capillaries as well as the formation of microvessel outgrowths in the rat aortic ring model of angiogenesis suggesting that β and γ-secretase activities are required during the angiogenic process. In addition, we observed that β and γ-secretase inhibitors suppress the growth of human brain and human lung adenocarcinoma tumors xenografted into nude mice, which are dependent on angiogenesis for their growth. Among the γ-secretase inhibitors tested, JLK-6 (a γ-secretase inhibitor which does not affect Notch processing (Petit et al., 2001)) also appears to reduce angiogenesis in vitro and to inhibit the growth and vascularization of human lung tumor xenografts suggesting the inhibition of angiogenesis observed following γ-secretase inhibition by JLK-6 is Notch independent.

At that point, we do not know the mechanisms responsible for the anti-angiogenic and anti-tumoral properties of β and γ-secretase. The fact that both β and γ-secretase inhibitors are able to inhibit angiogenesis suggests that β and γ-secretase or substrates/products of both enzymes may play a critical role during angiogenesis. γ-Secretase is known to process several proteins including Notch, LDL receptor-related protein, CD44, E-cadherin, and ErbB-4, which are all known to play some important regulatory functions during angiogenesis. One possibility is that some γ-secretase inhibitors, by affecting the Notch/β-catenin pathway, may disrupt the angiogenic process. CD44, another substrate for γ-secretase (Lammich et al., 2002) has also been shown to play a role in angiogenesis (Blaschuk and Rowlands, 2000). Additionally, ErbB-4 another substrate of γ-secretase is known to play a role in tumor angiogenesis by controlling VEGF expression (Yen et al., 2002). E-cadherin, an important regulator of angiogenesis (Blaschuk and Rowlands, 2000; Liao et al., 2000), is also cleaved by γ-secretase (Marambaud et al., 2002). It is therefore conceivable that γ-secretase inhibitors by altering the processing of many proteins involved in angiogenesis may oppose angiogenesis and tumor growth. The anti-angiogenic activity of β-secretase inhibitors is more surprising and suggests that an alteration of the β-amyloid precursor protein processing may impair angiogenesis. It has been hypothesized that the β-amyloid precursor protein and/or secreted forms of amyloid precursor protein may have a fundamental function in tumor cells, perhaps being involved in cellular growth, differentiation and tumorigenesis since tumor cells generally express APP mRNA and also secrete fragments of the β-amyloid precursor protein with a Kunitz-type serine proteinase inhibitor domain as their main cellular serine proteinase inhibitor (Kataoka et al., 1995; Seguchi et al., 1999; Meng et al., 2001; Nakagawa et al., 1999). Therefore, modulating β-amyloid precursor protein processing by using β-secretase or γ-secretase inhibitors may also have an impact on tumor growth. Interactions between endothelial cells and their surrounding extracellular matrix also play a crucial role during angiogenesis. It is possible that β and γ-secretase inhibitors may also inhibit other proteases responsible for matrix remodeling, hence inhibiting the angiogenic process and halting tumor growth. Altogether, our data reveal for the first time that both β and γ-secretase inhibitors can inhibit angiogenesis and tumor growth suggesting that β and γ-secretases play a key role in angiogenesis. β and γ-secretase inhibitors may therefore constitute an attractive class of compounds for the treatment of disorders associated with excessive angiogenesis such as cancer, psoriasis and diabetic retinopathy.

Acknowledgements

We extend our gratitude to Diane and Robert Roskamp for their generous support, which made work possible.

References

Abbenante, G., Kovacs, D.M., Leung, D.L., Craik, D.J., Tanzi, R.E., Fairlie, D.P., 2000. Inhibitors of beta-amyloid formation based on the beta-secretase cleavage site. Biochem. Biophys. Res. Commun. 268, 133–135.

Artacho-Perula, E., Roldan-Villalobos, R., 1995. Estimation of capillary length density in skeletal muscle by unbiased stereological methods: II. Use of vertical slices of unknown thickness. Anat. Rec. 241, 345–352.

Blaschuk, O.W., Rowlands, T.M., 2000. Cadherins as modulators of angiogenesis and the structural integrity of blood vessels. Cancer Metastasis Rev. 19, 1–5.

Braendgaard, H., Gundersen, H.J., 1986. The impact of recent stereological advances on quantitative studies of the nervous system. J. Neurosci. Methods 18, 39–78.

Brou, C., Logeat, F., Gupta, N., Bessia, C., LeBail, O., Doedens, J.R., Cumano, A., Roux, P., Black, R.A., Israel, A., 2000. A novel proteolytic cleavage involved in Notch signaling: the role of the disintegrin-metalloprotease TACE. Mol. Cell 5, 207–216.

Cao, X., Sudhof, T.C., 2001. A transcriptionally active complex of APP with Fe65 and histone acetyltransferase Tip60. Science 293, 115–120.

Carmeliet, P., 2000. VEGF gene therapy: stimulating angiogenesis or angioma-genesis? Nat. Med. 6, 1102–1103.

Clarke, K., Lee, F.T., Brechbiel, M.W., Smyth, F.E., Old, L.J., Scott, A.M., 2000. Therapeutic efficacy of anti-Lewis(y) humanized 3S193 radioimmunotherapy in a breast cancer model: enhanced activity when combined with taxol chemotherapy. Clin. Cancer Res. 6, 3621–3628.

Corada, M., Zanetta, L., Orsenigo, F., Breviario, F., Lampugnani, M.G., Bernasconi, S., Liao, F., Hicklin, D.J., Bohlen, P., Dejana, E., 2002. A monoclonal antibody to vascular endothelial–cadherin inhibits tumor angiogenesis without side effects on endothelial permeability. Blood 100, 905–911.

De Strooper, B., Annaert, W., Cupers, P., Saftig, P., Craessaerts, K., Mumm, J.S., Schroeter, E.H., Schrijvers, V., Wolfe, M.S., Ray, W.J., Goate, A., Kopan, R., 1999. A presenilin-1-dependent gamma-secretase-like protease mediates release of Notch intracellular domain. Nature 398, 518–522.

Dovey, H.F., John, V., Anderson, J.P., Chen, L.Z., de Saint Andrieu, P., Fang, L.Y., Freedman, S.B., Folmer, B., Goldbach, E., Holsztynska, E.J., Hu, K.L., Johnson-Wood, K.L., Kennedy, S.L., Kholodenko, D., Knops, J.E., Latimer, L.H., Lee, M., Liao, Z., Lieberburg, I.M., Motter, R.N., Mutter, L.C., Nietz, J., Quinn, K.P., Sacchi, K.L., Seubert, P.A., Shopp, G.M., Thorsett, E.D., Tung, J.S., Wu, J., Yang, S., Yin, C.T., Schenk, D.B., May, P.C., Altstiel, L.D., Bender, M.H., Boggs, L.N., Britton, T.C., Clemens, J.C., Czilli, D.L., Dieckman-McGinty, D.K., Droste, J.J., Fuson, K.S., Gitter, B.D., Hyslop, P.A., Johnstone, E.M., Li, W.Y., Little, S.P., Mabry, T.E., Miller, F.D., Audia, J.E., 2001. Functional gamma-secretase inhibitors reduce beta-amyloid peptide levels in brain. J. Neurochem. 76, 173–181.

Forloni, G., Demicheli, F., Giorgi, S., Bendotti, C., Angeretti, N., 1992. Expression of amyloid precursor protein mRNAs in endothelial, neuronal and glial cells: modulation by interleukin-1. Brain Res. Mol. Brain Res. 16, 128–134.

Greenwald, I., 1998. LIN-12/Notch signaling: lessons from worms and flies. Genes Dev. 12, 1751–1762.

Hardy, J., Selkoe, D.J., 2002. The amyloid hypothesis of Alzheimer's disease: progress and problems on the road to therapeutics. Science 297, 353–356.

Herreman, A., Hartmann, D., Annaert, W., Saftig, P., Craessaerts, K., Serneels, L., Umans, L., Schrijvers, V., Checler, F., Vanderstichele, H., Baekelandt, V., Dressel, R., Cupers, P., Huylebroeck, D., Zwijsen, A., Van Leuven, F., De Strooper, B., 1999. Presenilin 2 deficiency causes a mild pulmonary phenotype and no changes in amyloid precursor protein processing but enhances the embryonic lethal phenotype of presenilin 1 deficiency. Proc. Natl. Acad. Sci. U. S. A. 96, 11872–11877.

Hong, L., Koelsch, G., Lin, X., Wu, S., Terzyan, S., Ghosh, A.K., Zhang, X.C., Tang, J., 2000. Structure of the protease domain of memapsin 2 (beta-secretase) complexed with inhibitor. Science 290, 150–153.

Kataoka, H., Seguchi, K., Iwamura, T., Moriyama, T., Nabeshima, K., Koono, M., 1995. Reverse-zymographic analysis of protease nexin-II/amyloid beta protein precursor of human carcinoma cell lines, with special reference to the grade of differentiation and metastatic phenotype. Int. J. Cancer 60, 123–128.

Kim, D.Y., Ingano, L.A., Kovacs, D.M., 2002. Nectin-1alpha, an immunoglobulin-like receptor involved in the formation of synapses, is a substrate for presenilin/gamma-secretase-like cleavage. J. Biol. Chem. 277, 49976–499781.

Kubota, Y., Kleinman, H., Martin, G., Lawley, T., 1988. Role of laminin and basement membrane in the morphological differentiation of human endothelial cells into capillary-like structures. J. Cell Biol. 107, 1589–1598.

Lammich, S., Okochi, M., Takeda, M., Kaether, C., Capell, A., Zimmer, A.K., Edbauer, D., Walter, J., Steiner, H., Haass, C., 2002. Presenilin-dependent intramembrane proteolysis of CD44 leads to the liberation of its intracellular domain and the secretion of an Abeta-like peptide. J. Biol. Chem. 277, 44754–44759.

LaVoie, M.J., Selkoe, D.J., 2003. The Notch ligands, Jagged and Delta, are sequentially processed by alpha-secretase and presenilin/gamma-secretase and release signaling fragments. J. Biol. Chem. 278, 34427–34437.

Leissring, M.A., Murphy, M.P., Mead, T.R., Akbari, Y., Sugarman, M.C., Jannatipour, M., Anliker, B., Muller, U., Saftig, P., De Strooper, B., Wolfe, M.S., Golde, T.E., LaFerla, F.M., 2002. A physiologic signaling role for the gamma -secretase-derived intracellular fragment of APP. Proc. Natl. Acad. Sci. U. S. A. 99, 4697–4702.

Liao, F., Li, Y., O'Connor, W., Zanetta, L., Bassi, R., Santiago, A., Overholser, J., Hooper, A., Mignatti, P., Dejana, E., Hicklin, D.J., Bohlen, P., 2000. Monoclonal antibody to vascular endothelial–cadherin is a potent inhibitor of angiogenesis, tumor growth, and metastasis. Cancer Res. 60, 6805–6810.

Mailhos, C., Modlich, U., Lewis, J., Harris, A., Bicknell, R., Ish-Horowicz, D., 2001. Delta4, an endothelial specific notch ligand expressed at sites of physiological and tumor angiogenesis. Differentiation 69, 135–144.

Marambaud, P., Shioi, J., Serban, G., Georgakopoulos, A., Sarner, S., Nagy, V., Baki, L., Wen, P., Efthimiopoulos, S., Shao, Z., Wisniewski, T., Robakis, N.K., 2002. A presenilin-1/gamma-secretase cleavage releases the E-cadherin intracellular domain and regulates disassembly of adherens junctions. EMBO J. 21, 1948–1956.

May, P., Reddy, Y.K., Herz, J., 2002. Proteolytic processing of low density lipoprotein receptor-related protein mediates regulated release of its intracellular domain. J. Biol. Chem. 277, 18736–18743.

Meng, J.Y., Kataoka, H., Itoh, H., Koono, M., 2001. Amyloid beta protein precursor is involved in the growth of human colon carcinoma cell in vitro and in vivo. Int. J. Cancer 92, 31–39.

Murakami, D., Okamoto, I., Nagano, O., Kawano, Y., Tomita, T., Iwatsubo, T., De Strooper, B., Yumoto, E., Saya, H., 2003. Presenilin-dependent gamma-secretase activity mediates the intramembranous cleavage of CD44. Oncogene 22, 1511–1516.

Nakagawa, T., Kabuto, M., Kubota, T., Kodera, T., Sato, K., 1999. Production of amyloid beta protein precursor as a proteinase inhibitor by human astrocytic tumors. Anticancer Res. 19, 2963–2968.

Nakajima, M., Yuasa, S., Ueno, M., Takakura, N., Koseki, H., Shirasawa, T., 2003. Abnormal blood vessel development in mice lacking presenilin-1. Mech. Dev. 120, 657–667.

Ni, C.Y., Murphy, M.P., Golde, T.E., Carpenter, G., 2001. Gamma-secretase cleavage and nuclear localization of ErbB-4 receptor tyrosine kinase. Science 294, 2179–2181.

Nicosia, R.F., Bonanno, E., Villaschi, S., 1992. Large-vessel endothelium switches to a microvascular phenotype during angiogenesis in collagen gel culture of rat aorta. Atherosclerosis 95, 191–199.

Nicosia, R.F., Lin, Y.J., Hazelton, D., Qian, X., 1997. Endogenous regulation of angiogenesis in the rat aorta model. Role of vascular endothelial growth factor. Am. J. Pathol. 151, 1379–1386.

Ott, M.O., Bullock, S.L., 2001. A gene trap insertion reveals that amyloid precursor protein expression is a very early event in murine embryogenesis. Dev. Genes Evol. 211, 355–357.

Paris, D., Townsend, K., Quadros, A., Humphrey, J., Sun, J., Brem, S., Wotoczek-Obadia, M., Quadros, M., DelleDonne, A., Patel, N., Obregon, F., Crescentini, R., Abdullah, L., Coppola, D., Rojiani, A., Crawford, F., Sebti, S., Mullan, M., 2004. Inhibition of angiogenesis by Aβ peptides. Angiogenesis 7, 75–85.

Petit, A., Bihel, F., Alves da Costa, C., Pourquie, O., Checler, F., Kraus, J.L., 2001. New protease inhibitors prevent gamma-secretase-mediated production of Abeta40/42 without affecting Notch cleavage. Nat. Cell Biol. 3, 507–511.

Pinnix, I., Musunuru, U., Tun, H., Sridharan, A., Golde, T., Eckman, C., Ziani-Cherif, C., Onstead, L., Sambamurti, K., 2001. A novel gamma -secretase assay based on detection of the putative C-terminal fragment-gamma of amyloid beta protein precursor. J. Biol. Chem. 276, 481–487.

Pourquie, O., 2003. The segmentation clock: converting embryonic time into spatial pattern. Science 301, 328–330.

Roberts, S.B., 2002. Gamma-secretase inhibitors and Alzheimer's disease. Adv. Drug Deliv. Rev. 54, 1579–1588.

Sastre, M., Steiner, H., Fuchs, K., Capell, A., Multhaup, G., Condron, M.M., Teplow, D.B., Haass, C., 2001. Presenilin-dependent gamma-secretase processing of beta-amyloid precursor protein at a site corresponding to the S3 cleavage of Notch. EMBO Rep. 2, 835–841.

Savani, R.C., Cao, G., Pooler, P.M., Zaman, A., Zhou, Z., DeLisser, H.M., 2001. Differential involvement of the hyaluronan (HA) receptors CD44 and receptor for HA-mediated motility in endothelial cell function and angiogenesis. J. Biol. Chem. 276, 36770–36778.

Seguchi, K., Kataoka, H., Uchino, H., Nabeshima, K., Koono, M., 1999. Secretion of protease nexin-II/amyloid beta protein precursor by human colorectal carcinoma cells and its modulation by cytokines/growth factors and proteinase inhibitors. Biol. Chem. 380, 473–483.

Shearman, M.S., Beher, D., Clarke, E.E., Lewis, H.D., Harrison, T., Hunt, P., Nadin, A., Smith, A.L., Stevenson, G., Castro, J.L., 2000. L-685,458, an aspartyl protease transition state mimic, is a potent inhibitor of amyloid beta-protein precursor gamma-secretase activity. Biochemistry 39, 8698–8704.

Shen, J., Bronson, R.T., Chen, D.F., Xia, W., Selkoe, D.J., Tonegawa, S., 1997. Skeletal and CNS defects in Presenilin-1-deficient mice. Cell 89, 629–639.

Simons, E.R., Marshall, D.C., Long, H.J., Otto, K., Billingslea, A., Tibbles, H., Wells, J., Eisenhauer, P., Fine, R.E., Cribbs, D.H., Davies, T.A., Abraham, C.R., 1998. Blood brain barrier endothelial cells express candidate amyloid precursor protein-cleaving secretases. Amyloid 5, 153–162.

Sinha, S., Lieberburg, I., 1999. Cellular mechanisms of beta-amyloid production and secretion. Proc. Natl. Acad. Sci. U. S. A. 96, 11049–11053.

Vassar, R., 2002. Beta-secretase (BACE) as a drug target for Alzheimer's disease. Adv. Drug Deliv. Rev. 54, 1589–1602.

Vassar, R., Bennett, B.D., Babu-Khan, S., Kahn, S., Mendiaz, E.A., Denis, P., Teplow, D.B., Ross, S., Amarante, P., Loeloff, R., Luo, Y., Fisher, S., Fuller, J., Edenson, S., Lile, J., Jarosinski, M.A., Biere, A.L., Curran, E., Burgess, T., Louis, J.C., Collins, F., Treanor, J., Rogers, G., Citron, M., 1999. Beta-secretase cleavage of Alzheimer's amyloid precursor protein by the transmembrane aspartic protease BACE. Science 286, 735–741.

Yen, L., Benlimame, N., Nie, Z.R., Xiao, D., Wang, T., Moustafa, A.E., Esumi, H., Milanini, J., Hynes, N.E., Pages, G., Alaoui-Jamali, M.A., 2002. Differential regulation of tumor angiogenesis by distinct ErbB homo- and heterodimers. Mol. Biol. Cell 13, 4029–4044.

Zhong, T.P., Childs, S., Leu, J.P., Fishman, M.C., 2001. Gridlock signalling pathway fashions the first embryonic artery. Nature 414, 216–220.

Zimrin, A.B., Pepper, M.S., McMahon, G.A., Nguyen, F., Montesano, R., Maciag, T., 1996. An antisense oligonucleotide to the notch ligand jagged enhances fibroblast growth factor-induced angiogenesis in vitro. J. Biol. Chem. 271, 32499–32502.